Glassy Dynamics, Aging in Mobility, and Structural Relaxation of Strongly Adsorbed Polymer Films: Corrugation or Confinement?

Debashish Mukherji*

Department of Physics & Astronomy, University of Western Ontario, London, Ontario N6A 3K7, Canada

Martin H. Müser*

Department of Applied Mathematics, University of Western Ontario, London, Ontario N6A 5B7, Canada

Received November 29, 2006; Revised Manuscript Received January 17, 2007

ABSTRACT: A molecular dynamics simulation (MD) of a generic model for polymers adsorbed on a discrete surface is presented. We investigate the effect of surface roughness on the film's diffusion constant, its influence on aging, and other properties. The model reproduces many experimentally observed features such as logarithmic aging of structural properties with time, a power law aging of the diffusion constant D, and the anomalous dependence of mobility with surface coverage. It is shown that the glassy dynamics is intimately linked to the roughness, which can be controlled by changing the interaction potential between surface atoms and adsorbed particles. We observe a logarithmic increase in the structure factor with aging time and a power law decay in D only if the corrugation is sufficiently high. For a smooth surface, no such time dependence is observed, even if adhesion and thus confinement is increased. We also address the question as to why the mobility of adsorbed polymers can initially increase with surface coverage Γ when Γ is low.

1. Introduction

Dynamics of polymers have attracted a great deal of experimental and theoretical interest. The focus has traditionally been on diffusion of polymers in the bulk.[1−4] In recent years, considerable effort has also been made to understand polymer dynamics on surfaces and interfaces, because these dynamics impose challenging problems in their fundamental understanding[5−8] and also have important technological applications.[9,10] On the theoretical and computational side, particular attention has been paid to the question of how the lateral diffusion coefficient D scales with the degree of polymerization N at a dilute surface coverage.[5,11−16] Extensive experimental work has also been done in particular with fluorescence spectroscopy.[6,7,17,18] This includes an analysis of how the diffusion coefficient of DNA nucleotides on lipid bilayers scales with the number of base pairs.[19,20]

To the best of our knowledge, most studies of polymer diffusion on surfaces have been performed at a dilute surface coverage concentration. However, it is also important to address the effect of increasing surface coverage on the diffusion coefficient and to understand how the increasing interaction between neighboring polymer chains affect their lateral mobility. In a recent experiment, an unpredicted dependence of D on surface coverage Γ was found:[21] $D(\Gamma)$ first increased monotonically with Γ from its value associated with dilute concentrations ($\Gamma \ll 1$) to a maximum value. At a given threshold concentration Γ^*, D decreased rather abruptly in such a manner that a graph of $D(\Gamma)$ resembled the letter Λ. Because of this similarity, the observed behavior was termed a Λ-shape anomaly in the diffusion coefficient.[22] In the experiments,[21] polyethylene glycol (PEG) was deposited from an aqueous solution onto fused silica surfaces with hydrophobic termination. Diffusion was measured with fluorescence spectroscopy in which the signal of fluorescent labels, which were attached to the PEG molecules, was detected.

The perhaps counter-intuitive Λ-shape anomaly could be reproduced in a recent molecular dynamics study by the authors of the present paper:[22] On the basis of simulations of a generic model for polymer−polymer and polymer−substrate interactions, it was found that at $\Gamma < \Gamma^*$, deposited polymers have the tendency to instantaneously form single-layered pancake structures, while double layers are preferentially formed for $\Gamma > \Gamma^*$. The double-layer structures give the polymers more flexibility to adapt to the substrate corrugation. This increases their energy barrier for lateral motion and is thus consistent with the much reduced value of D at larger concentration.[22]

An essential part in modeling the concentration dependence of the diffusion constant in ref 22 was to *explicitly* include the substrate's surface corrugation. The same model[16] reproduced the experimentally observed scaling $D \sim N^{-1.5}$ [6,7] for single−polymer diffusion on solid surfaces. Previously, most simulations had been based on attractive, hard-wall, but perfectly smooth boundaries. In these cases, diffusion of polymers can only be hindered by other polymers, however, the substrate cannot exert a lateral force on a polymer film, due to translational invariance. Thus, addressing the question of how a substrate manages to exert frictional forces onto adsorbed layers in general,[23] and polymers in particular, is a key task if we want to understand polymer diffusion on surfaces. For simple fluids adsorbed on crystalline substrates, it is well understood how density modulations are imprinted into the adsorbed layer and how this affects flow boundary conditions.[23−25] One of the difference between simple fluids and adsorbates consisting of chain molecules may be how a second layer would affect the diffusion constant (or "slip time'') of the film. In a simple fluid, one would expect the second layer to typically reduce the substrate's imprint, that is, if the intrinsic length scales in the

* Corresponding author. E-mail: dmukherj@uwo.ca. E-mail: mmuser@uwo.ca. Web: http://publish.uwo.ca/mmuser/.

10.1021/ma0627370 CCC: $37.00
Published on Web 02/10/2007

fluid differ from those of the substrate. The opposite trend appears to hold for chain molecules, where locking increases with an increased number of layers, as suggested in the precedent paragraph.

It had been argued that the experimentally observed diffusion anomaly in adsorbed polymer films may be due to nonequilibrium effects.[8] Explicitly modeling the deposition process in the simulations,[22] which allowed for the occurrence of metastable states and thus out-of-equilibrium situations, turned out to be another important part in interpreting the experiments by Zhao and Granick;[21] i.e., the initially formed structure has a crucial influence on the long-time dynamics. If a system is initially not in thermal equilibrium, it will attempt to reach thermodynamic equilibrium via a process typically referred to as structural relaxation or aging.[26−28] During this process not only structural or static properties such as density and internal energy are time dependent but also dynamical properties.

There has not only been a long history of studying aging in bulk polymers but also in adsorbed polymer films.[29,30] For example, the sudy of kinetics of adsorption−desorption of the polymer chains near surfaces,[31] film thickness dependence of physical aging,[32] the aging of properties such as refractive index of thin glassy polymer films, which was used to track the physical aging, more specifically the rate of permiability loss and the densification of the thin glassy film was studied.[33,34] Recently, logarithmic structural relaxation was obeserved experimentally not only for bulk systems but also for confined polymeric systems.[28] Dynamics could be spatially ressolved near surfaces, near interfaces, and in between owing to the use of fluorescence spectroscopy.

None of the above-mentioned studies, except refs 16 and 22 explicitly addressed the question of how the substrate manages to imprint its (atomic-scale) corrugation into the film and how this imprint affects the aging in the film, in particular the aging of polymer diffusion. Investigating this matter is the central topic of this paper. This can be done particularly well in computer simulations, because roughness can be changed at will in a continuous fashion.[35]

In this paper, we will also extend our analysis from previous work, in which crystalline substrates were used, to disordered surfaces. Specifically, it will be investigated whether single and double-layer formation also occurs spontaneously on disordered substrates for small and high concentration, respectively, and whether similar dynamical effects are observed as a function of film thickness as on crystalline substrates.

The reminder of this paper is organized as follows: In section 2, we sketch our methodology. Results for crystalline and amorphous surfaces are presented in sections 3 and 4, respectively. Conclusions are drawn in section 5.

2. Methodology

In this section, we discuss the model used in the MD simulations. In a nutshell, the model used is a well-known bead−spring model for polymers, which move on an essentially impenetrable surface with atomic-scale roughness. The following few aspects of our treatment will be described here: Interaction between monomers, modeling of the substrate, thermostating, and the deposition of the polymers onto the surface.

The interaction between monomers is based on a widely used, simple, and generic bead−spring model for polymers.[36] As this model has been used in an abundance of studies,[37] we summarize only its key ingredients: Individual monomers of the polymers interact with each other and with substrate atoms via a truncated 6−12 Lennard-Jones (LJ) potential, where unless stated otherwise the cutoff radius is chosen as $r_c = 2 \times 2^{1/6}\sigma$, where σ is the LJ interaction radius. When mimicking good solvent conditions, the LJ potential is cutoff where the 6−12 LJ potential has its minimum and shifted above so that it becomes continuous at the cutoff. For bad solvent conditions, the interaction radius is twice as large. Adjacent monomers in a polymer are connected via a finitely extensible nonlinear elastic potential (FENE). The parameters are chosen such that a reasonably large time step can be chosen, while bond crossing remains exceedingly unlikely to occur.[36] Typical unit time and length scales of this model are $\sigma = 0.5$ nm and $t_0 = 3$ ps, respectively. The unit of pressure is $p_0 = 40$ MPa. The degree of polymerization is $N = 10$. While the chain molecules are thus too short for entanglements, they are sufficiently long to show properties of linear chain molecules, e.g., the effects alluded to above, in particular the Λ-shape anomaly in the diffusion coefficient, cannot be observed for N less than 5. Moreover, the desorption dynamics of single polymer chains with N being on the order of 100 repeat units[16] resembles the desorption dynamics of the chains studied here. Thus, while our chain molecules classify better as *oligomer* than a *polymer*, they are still in the regime of flexible linear chain.

The substrate consists either of a two-dimensional hexagonal lattice, i.e., the (111) surface of a face-centered-cubic solid, or an amorphous layer. In both cases the substrate atoms are constrained to their lattice positions. For the hexagonal lattice, the nearest-neighbor spacing of substrate atoms is $d = 1.209$ σ, specifically, disordered surfaces were produced following the protocol described in ref 38. A liquid LJ fluid was quenched to small temperatures at high pressures. The resulting, dense glass was cut such that all atoms with a z-coordinate larger than a given value were discarded. Remaining atoms were kept so that a dense, amorphous layer was produced. The linear dimension of our substrate is roughly 37.5σ for both crystalline and amorphous systems. Periodic boundary conditions are applied in the (xy)-plane of the substrate. The interaction between monomers and substrate atoms is also a 6−12 LJ potential, with the long-range cutoff radius. Polymers are thus attracted to the substrate. Similar models for monomer-substrate interactions have been used previously to study the diffusion of two walls separated by polymers.[39] Here, however, we consider only one substrate and focus on the diffusion of the polymers rather than the diffusion of two confining walls. The surface coverage Γ is stated in terms of the ratio of number of monomers per unit surface element $\Delta A = \sigma^2$. A value of $\Gamma = 1$ corresponds roughly to a full monolayer coverage. Moreover, each substrate atom occupies an area of 1.26 ΔA.

Since the substrate atoms are constrained to their (ideal) positions, the motion of the polymers needs to be thermostated so that constant temperature conditions can be mimicked. For this purpose, we chose a Langevin thermostat which only acts on the motion in z direction, i.e., in the direction normal to the interface. The Langevin damping term is chosen sufficiently small so that its precise choice has no detectable effect on the measured quantities. The thermal energy is set to 0.5ϵ, which is sufficiently small to make the polymers stick to the surface, while it is still high enough to allow the polymers to diffuse laterally during the time span of the simulation. At this temperature, a bulk Lennard-Jones bead−spring system would show glassy dynamics.

Initial configurations are generated with the following protocol: The lateral and normal position of the first monomer unit in a polymer is chosen at random. The z coordinate is constrained to be within 1 and 5 σ away from the substrate.

Once the position of the first monomer unit is found, the remaining monomers of a molecule are generated via a random walk in which the bond length is kept fixed. The initial configuration is relaxed for a brief moment. During this relaxation, overlap of monomers is reduced but no structural changes occur on larger length scales. In all cases that we encountered, this protocol made the polymers adsorb to the surface within about the first two thousand MD time steps, i.e., no polymer was lost to the gas phase. Because of the strong polymer−substrate interaction, (isolated) polymers quickly adopt a flat configuration on the substrate, as soon as one monomer has experiences the attractive force from the substrate. We believe that this procedure reproduces the experimental deposition from solution reasonably well. Note that for the given model, chain molecules with $N = 70$ in good solvents and dilute concentrations also adsorb flat on surfaces and that any initially imposed bond crossing becomes unstable within a few 10^6 time steps.[16]

The equation of motion are integrated using fifth order predictor-corrector method with time step $\Delta t = 0.005t_0$. The simulations were usually equilibrated for 5×10^8 MD time steps, that is, $2.5 \times 10^6 t_0$ and in some cases for longer times. The system is then typically observed over another few 10^7 MD time steps (i.e., $5 \times 10^4 t_0$). During this time, observables such as the diffusion constant D and the static structure factor S(Q) are measured. The error bars for D and $S(Q)$ are typically on the order of 10%, which we estimated from running three or four runs with stochastically independent initial configurations. Owing to the length of individual runs, we were not in a position to produce more data. Moreover, due to the nonequilibrium nature of the dynamics, we only used one procedure to initialize the configurations and did not consider different thermalization schemes. When measuring time-dependent properties, the initial equilibration was sometimes chosen shorter then 5×10^8 MD time steps. Details are mentioned in the text whenever appropriate.

3. Results for Crystalline Surfaces

3.1. Observables. The time-dependent, mean-square displacement $C(\tau, t)$, defined here below, is a key quantity for the study of lateral diffusion of polymers on surfaces:

$$C(\tau,t) = \frac{1}{2N}\sum_{\alpha=1}^{2}\sum_{i=1}^{N}\langle[R_{i\alpha}(\tau) - R_{i\alpha}(\tau + t)]^2\rangle \qquad (1)$$

In this equation, $R_{i\alpha}(t)$ is the x or y component of the position of monomer i in a given polymer at time t and $\langle\bullet\rangle$ denotes an ensemble average over all molecules and potentially different initial microscopic realizations. The time τ indicates the age of the system, i.e., τ is set to zero at the moment where the polymers are released from the solution.

If the system has aged for an infinitely long time, it can be assumed to be in thermodynamic equilibrium, in which case the equilibrium time-dependent mean-square displacement can be defined as

$$C_{eq}(t) = \lim_{\tau\to\infty} C(\tau,t) \qquad (2)$$

From $C_{eq}(t)$ one can deduce the equilibrium diffusion constant D_{eq} via the equation

$$D_{eq} = \frac{1}{2}\lim_{\tau\to\infty}\frac{\partial C_{eq}(t)}{\partial t} \qquad (3)$$

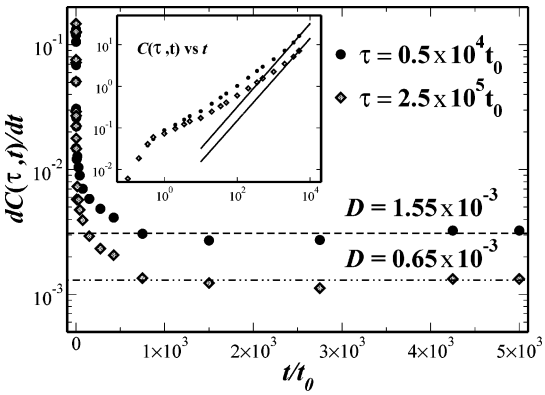

Figure 1. Time derivative of the mean-square displacement $C(\tau, t)$ for two samples with identical surface coverage $\Gamma = 0.072$ and different age τ. The plateau value of $\partial C(\tau, t)/\partial t$ can be interpreted as twice the nonequilibrium value of the diffusion constant. Inset: Original data of $C(\tau, t)$. The lines are power-law fits to $C(\tau, t)$ at the largest values of t. The fitted power law gives exponents close to unity indicating diffusive behavior.

If there is a clear time scale separation between slowly relaxing modes and fast modes, then it is possible to extend the definition of the diffusion constant to a nonequilibrium situation. For instance, if the quantity $D(\tau,t)$ defined as

$$D(\tau,t) = \frac{1}{2}\frac{\partial C(\tau,t)}{\partial t} \qquad (4)$$

then $D(\tau,t)$ may depend only very weakly on the precise choice of t as long as t is greater than the relaxation times τ_f associated with the fast modes but not greater than τ itself. This makes it possible to associate the value of $D(\tau,\tau_f \ll t < \tau)$ with a nonequilibrium diffusion constant in a system of age τ.

The inset of Figure 1 shows the original mean-square displacement function $C(\tau, t)$ for a sample at two ages τ. For both values of τ, it is possible to observe an initially ballistic regime at times $t/t_0 < 1$ in which $C(\tau, t) \propto t^2$, subdiffusive behavior for $1 < t/t_0 < 10^3$, and an apparently diffusive regime for $t/t_0 > 10^3$. This behavior is similar to regular dynamics in glassy polymer systems. The interesting feature of the behavior here is that the (apparent) prefactors in the diffusive regimes differ for the samples with different age.

The main part of Figure 1 shows the generalized diffusion constant $D(\tau, t)$. After a time $t = 1.5 \times 10^3$, there is only a virtually unnoticeable time dependence of $D(\tau, t)$, at least on a linear time scale, i.e., for the given values of τ, $D(\tau, t)$ remains constant within stochastic error in the interval $1.5 \times 10^3 \le t/t_0 \le 5 \times 10^3$. The value of the initial plateau in $\partial C(\tau, t)/\partial t$ is what will be referred to as the diffusion constant of a system at age τ.

Another central observable in this study is the orientationally averaged and time-dependent *static* structure factor $S(Q,\tau)$,[2]

$$S(Q,\tau) = \frac{1}{2\pi Q}\int \mathrm{d}^2Q'\delta(Q - |Q'|)S(Q',\tau) \qquad (5)$$

with

$$S(\mathrm{Q},\tau) = \frac{1}{N}\langle|\sum_{j=1}^{N}\mathrm{e}^{iQR_j(\tau)}|^2\rangle \qquad (6)$$

from which one can deduce to what degree the adsorbed polymer film manages to lock into the substrate's corrugation. In eq 6, an ensemble average over different initial microstructures is taken. The sum is taken over *all* monomers that are in direct

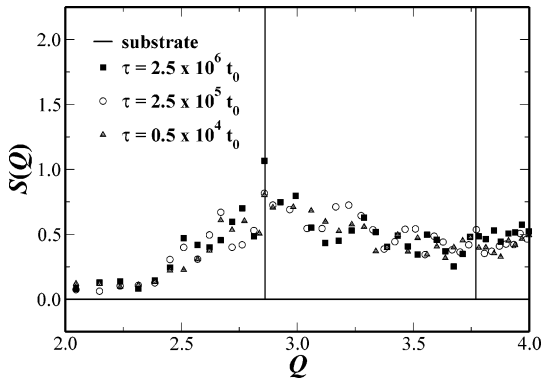

Figure 2. Static structure factor $S(Q)$ of the polymers calculated as a function of wave number Q for a single layer at $\Gamma = 0.072$. The three data sets corrspond to $S(Q)$ calculated after three different relaxation times τ. The vertical lines indicate the location of the substrate's reciprocal lattice vector.

contact within the substrate, e.g., when evaluating $S(Q,\tau)$ of a double-layer structure, only the bottom layer is included. The clear layering of the polymers in our simulations allows us to distinguish rather unambiguously whether a monomer belongs or does not belong to the first layer near the substrate. Also note that the "usual'' equilibrium static structure factor $S_{eq}(\mathbf{Q})$ does not depend on time or age, i.e., $S_{eq}(\mathbf{Q}) = \lim_{\tau\to\infty} S(Q,\tau)$.

In Figure 2, we show some representative data for $S(Q,\tau)$ for films with fixed $\Gamma = 0.072$ but different age τ. Values of Q are marked for which $Q = |\mathbf{G}|$, where $\mathbf{G}$ is the reciprocal lattice vector of the substrate. As τ increases, $S(Q = |G|,\tau)$ increases as well, indicating that the film better accommodates the substrate's corrugation as it ages. The aging of $S(Q = |G|,\tau)$ will be examined quantitatively in subsequent sections and figures.

3.2. Λ-Shape Anomaly in Polymer Lateral Diffusion: A Brief Overview. In our previous paper,[22] we provided a possible explanation for the experimentally observed anomalous behavior of the polymer lateral diffusion.[21] As discussed in the introduction, polymers below a threshold concentration Γ^* tend to form monolayers, while the spontaneous formation of double layers is preferred for $\Gamma > \Gamma^*$. Here, the word "spontaneous'' is meant to indicate a time span that is small compared to the time required to find thermal equilibrium, but of course long compared to characteristic vibrational times. Figure 3 shows the density profile of the islands for different surface coverages after a few hundred million MD time steps. It can be seen that at $\Gamma < \Gamma^*$ a single layer is found while for $\Gamma > \Gamma^*$, the density profile clearly shows a bimodal structure. Near the threshold concentrations, i.e., for $\Gamma = 0.214$, the density peak broadens indicating increased fluctuations of the monomers normal to the interface. In the next but two paragraphs, these fluctuations will be related to an increased mobility of the polymers.

Besides the broadening and the shifting of the density $n(z)$ near Γ^*, two small additional peaks occur in $n(z)$. At this point, we are not certain how to rationalize the origin of the two additional peaks. We can only speculate based on the available phenomenology. The extra peaks only occur for very large merged islands, see the section on film formation. It may be that the extra peaks are the consequence of fluctuations, which become favorable as the single-layered islands reach their instability point. The peak at the smaller value of z is located near the position where single monomers would reside if there were no geometric constraints due to the covalent bonds. We believe that large fluctuations are suppressed in the double layer, because the double layer is much more stable and thus is not

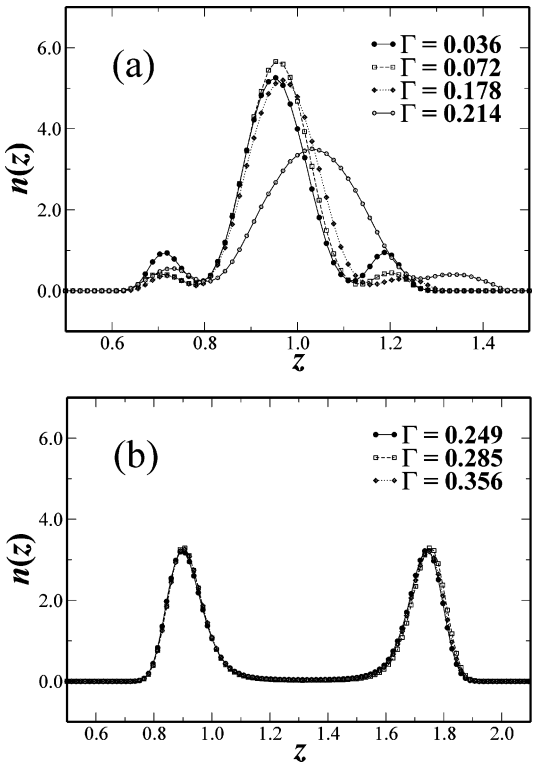

Figure 3. Density of the monomers $n(z)$ as a function of the distance z from the substrate. (a) $\Gamma < \Gamma^*$. In one case, $\Gamma = 0.214$, the surface coverage is only slightly below Γ^*. (b) $\Gamma > \Gamma^*$.

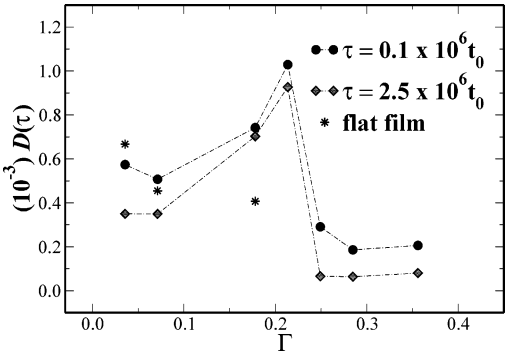

Figure 4. Lateral diffusion coefficient D as a function of surface coverage concentration Γ evaluated at two different ages τ of the film. Stars (flat film) refer to configurations in which all monomers have a fixed distance, i.e., $z = 0.9924$ in Lennard-Jones units from the substrate.

located near an instability point, which one could roughly associate with a spinodal. A more detailed analysis is beyond the scope of the present manuscript.

The double layers accommodate the substrate's corrugation more easily than the single layers, because they have additional geometric flexibility. This was demonstrated in our previous work[22] where the structure factor of the double layer was found to be much greater at the first reciprocal lattice vector of the substrate than that of a single layer. This geometric flexibility of the double layer leads to a sudden decrease in the diffusion constant D at $\Gamma = \Gamma^*$, as shown in Figure 4. Included is also information on how aging affects the anomalous behavior of thin-film polymer diffusion, i.e., for all investigated surface concentrations, aging decreases the mobility. The relative magnitude of the decrease in D appears to be larger for concentrations $\Gamma > \Gamma^*$, e.g., the diffusion constant drops to half of its value for $\Gamma = 0.356$ between the time $0.1 \times 10^6 t_0$ and $2.5 \times 10^6 t_0$.

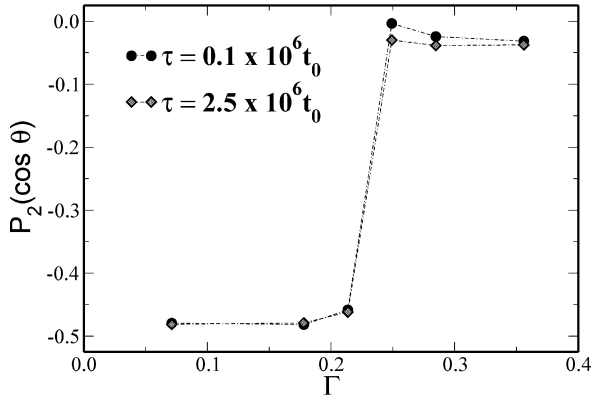

Figure 5. Second Legendre polynomial of the out-of-plane angle θ as a function of polymer surface concentration Γ, which is measured in number of monomers per unit surface area. The two curves corresponds to two samples with different ages. Lines are drawn to guide the eye.

It is interesting to note that D increases with Γ as long as single layers form. In our previous paper,[22] we had speculated that the increased mobility is due to increased fluctuations of the monomers normal to the interface when Γ approaches Γ^* from below. To test this conjecture, simulations were run in which the z positions of the monomers were constrained to a fixed value ($z_i = 0.9924\sigma$ for all monomers i). Surface coverages $\Gamma = 0.0356$, 0.0712, and 0.178 were considered. The value of $z_i = 0.9924\sigma$ corresponds to the expectation value of z_i in simulations of unconstrained monomers at $\Gamma = 0.178$. With fixed z coordinates, D *decreased* with Γ for both unrelaxed and aged structures from 0.67×10^{-3} (unrelaxed) and 0.47×10^{-3} (relaxed) at $\Gamma = 0.0356$ to 0.41×10^{-3} (unrelaxed) and 0.38×10^{-3} (relaxed) at $\Gamma = 0.178$.

Coming back to the abrupt decrease in D at around $\Gamma = 0.2$, it may be important to note that the double-layer structures do not consist of one pancake lying on top of another one. Instead, there is a lot of zigzag arrangements of the covalent bonds that often connect one monomer in the top with another one in the bottom layer. This is demonstrated in Figure 5, in which the average orientation of the monomer−monomer bond is shown using second-order Legendre polynomial

$$P_2(\cos\theta) = \frac{1}{2}(3\langle\cos^2\theta\rangle - 1) \qquad (7)$$

where θ is the angle between individual covalent bond and the direction normal to the surface, and the average is taken over all bonds and all the time. This quantity $P_2(\cos\theta)$ can be seen as an order parameter for the bond orientation: If all bonds are perpendicular to the surface, then $P_2(\cos\theta) = 1$. If bonds are random, then $P_2(\cos\theta) = 0$, while planar bonds lead to $P_2(\cos\theta) = -1/2$. Thus, Figure 5 indicates that the bonds are predominantly planar for $\Gamma < \Gamma^*$, while they have no ascertainable preference direction for $\Gamma > \Gamma^*$.

We believe that the zigzag pattern of the bonds is essential to allow the polymers to more flexibly accommodate the substrate's corrugation. If most bonds were confined to be parallel to the interface, it would be difficult for the polymers to lock into the substrate's registry, mainly due to the incompatibility of intrinsic length scales in the polymer film and that in the substrate, i.e., the distance between neighbored wall atoms is 1.204σ, while that between covalently bonded is around 0.96σ. Note that this qualitative argument does not rely on the precise choice of parameters, but only on the incompatibility of length scales, which in most cases should be given.

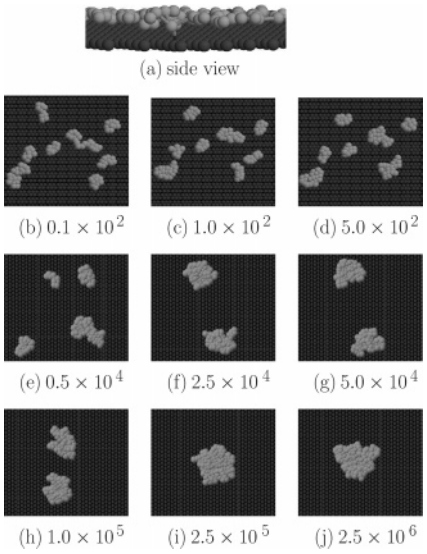

Figure 6. Snapshots of the film formation of an adsorbed polymer film for $\Gamma = 0.072$. Part a is a side view of the film at large times; all other parts reflect films of the indicated age τ/t_0.

While this paper is mainly concerned with the analysis of how corrugation affects diffusion of chain molecules on surfaces, we do not mean to suggest that adhesion does not play a role. Energy barriers certainly increase with the adhesive load (at fixed corrugation), but we consider this to be a well-know fact. Increased adhesion will certainly slow down the dynamics and hence reduce the diffusion constant. Moreover, increased adhesion will reduce the propensity of the polymers to form double-layered structures and thus increase Γ^*. We tested these assumption by running simulations where all parameters were identical as those of the default model, except for the Lennard-Jones, surface−polymer interaction strength ϵ_{sp}, which was reduced to $^1/_2$, i.e., half the default value. The outcome of these calculations showed the expected trends, that is, the diffusion constants increased by about a factor of 3 in either regime and Γ^* was reduced by 25%.

3.3. Film Formation. It had been argued that nonequilibrium effects in polymer deposition on surfaces may be dominant if the surface monomer sticking energy is greater than k_BT.[8] For the experimental system that motivated the current theoretical study, it was estimated that the sticking energy is k_BT,[21] which would suggest fluid dynamics. However, depending on the details of the surface, the rule of thumb mentioned in ref 8 may have to be altered. In fact, the discontinuity of the lateral diffusion coefficient at Γ^* supports the speculation that the system may not be in equilibrium. In full equilibrium, one would not expect such a discontinuity, or at least, in the case of a first-order phase transition, one would expect to be able to obtain information on the hysteresis. This hysteresis has not yet been explored experimentally.

In our simulations, the double layer structures are energetically distinctly more favorable than the single layers. We therefore believe that the film would probably have an increased propensity to form double layers also in the regime below Γ^*, if larger system sizes and much longer simulation times were computationally feasible. However, from observing the time evolution of the film formation, we conclude that the single-layer islands remain in a metastable equilibrium for extended periods of times, potentially even on experimental time scales.

The nonequilibrium or metastable character of the islands is clearly evidenced by snapshots of the simulations. Figures 6 and 7 show the time evolution of the film formation. Each of

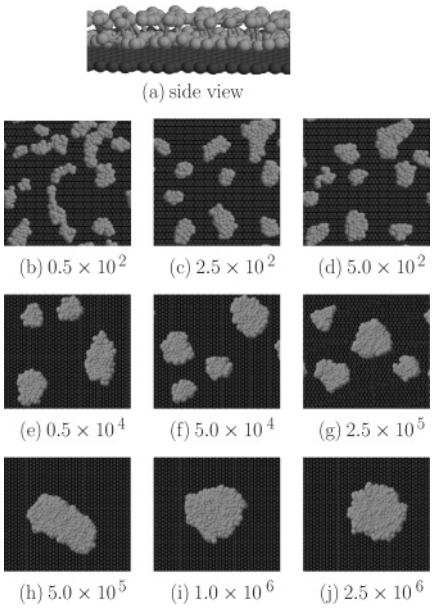

Figure 7. Similar to Figure 6, however, for $\Gamma = 0.278$.

the two figures has a side view at an elevated age of the islands and top views during the film formation at different ages of the film.

A remarkable feature of the simulation is that at the small deposition rate, the single-layer island, which has a net number of 100 monomers, remains stable up to an age of $\tau = 2.5 \times 10^6 t_0$. Conversely, at the elevated value of Γ, islands of much smaller size have generated at very small times, e.g., the smallest island in Figure 7b only contains 20 monomers whereas the largest island in Figure 7b has 110 monomers. Since the only difference between the underlying simulations of the discussed figures is the (initial) deposition, it seems to be evident that the initial preparation of the island and the way in which the polymers are deposited onto the surface play a dominant role in the later structural and thus dynamical properties of the islands.

It is interesting to note that the double-layers have the larger tendency to be spherical, which one can see with the bare eye. This observation can easily be understood from energetic considerations of the contact line: In a simple mean-field picture, the line tension of double layer structures would be twice as large as that of single layers. Part of the aging process in the double layer structure appears to be an approach to more spherical shapes with increasing age.

3.4. Time Dependence of Observables with Default Surface Roughness. In the following, we will be concerned with the time dependence of the structure factor and the diffusion constant. As argued qualitatively in the Introduction and the previous section, the dynamics of the polymer film are intimately connected to the degree with which it is able to adjust to the surface corrugation. It will therefore be instructive to ascertain how the film's structure factor evolves with time and whether the aging in the structure factor can be correlated with a slowing down in the diffusion.

We will investigate the aging of the time-dependent structure factor $S(G,\tau)$, where G is the absolute value of the substrate's smallest, nonzero reciprocal lattice vector. Results for two surface coverages, one for $\Gamma < \Gamma^*$ and one for $\Gamma > \Gamma^*$, are shown in Figure 8. In this figure, it can be observed that both single and double layer islands adjust their corrugation to the substrate as they relax toward (metastable) equilibrium.

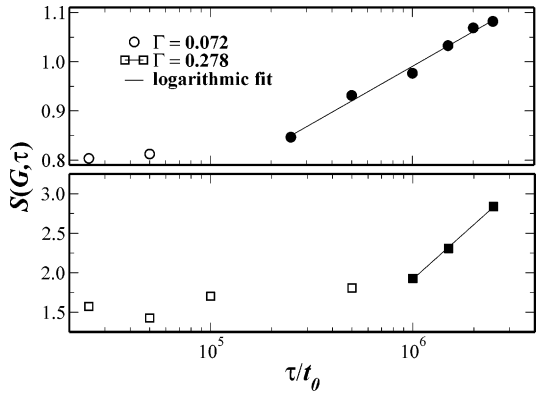

Figure 8. Structure factor $S(G,\tau)$ calculated near the first reciprocal lattice vector G of the substrate as a function of time τ for two different surface coverages Γ. $\Gamma = 0.072$ (circles) corresponds to single layer and $\Gamma = 0.278$ (squares) to double layers. Solid symbols refer to data in which the islands have merged completely, while open symbols reflect disconnected islands. Lines reflect fits based on eq 8.

A closer investigation of the $S(G,\tau)$ curve reveals that on logarithmic time scales, there is only a slight increase in $S(G,\tau)$ initially. However, if only data is considered for which all islands have merged to one blob, $S(G,\tau)$ appears to increase logarithmically with time τ; e.g., in Figure 6 the large island is formed after approximately $2.5 \times 10^5 t_0$, which coincides with the increase of $S(G,\tau)$ on logarithmic time scales. The observed behavior is reminiscent of aging effects in "confined'' glassy polymeric systems,[28] which could be described over a large time window with the help of the following law

$$S(\mathbf{G},\tau) = S_0(\mathbf{G}) \ln\left(\frac{\tau}{\tau_0}\right) \tag{8}$$

where τ_0 is a constant with the unit of time.

As argued previously,[22] lateral forces can only be exerted on polymer films if the translational invariance is broken in lateral direction. To leading-order contribution,[22,38] one can assume that there is a lateral energy barrier ΔE_b due to the substrate corrugation that is linear to the structure factor of the film evaluated at the first reciprocal lattice vector, i.e., $\Delta E_b \propto S(G)$ or if we allow for the time dependence of all properties, then,

$$\Delta E_b(\tau) \propto S(G,\tau) \tag{9}$$

A simple Arrhenius-type activation picture in which $D \propto \exp(-\Delta E_b/k_B T)$ would thus result in the following dependence of D on the (time-dependent) structure factor:

$$D\{S(\mathbf{G},\tau)\} = D_0 \mathrm{e}^{-\alpha S(\mathbf{G},\tau)/k_B T} \tag{10}$$

where α is a proportionality coefficient. Inserting the time dependence for $S(\mathbf{G},\tau)$ from eq 8 into eq 10 yields the explicit time dependence of the diffusion coefficient, which can be written as the following power law:

$$D(\tau) = D_0 \left(\frac{\tau}{\tau_0}\right)^{-\alpha S_0(G)/k_B T} \tag{11}$$

A power law behavior of D with τ is indeed found in the simulations as demonstrated in Figure 9. Given this result and Figure 8, the exponential dependence of D on $S(G)$ appears to be validated.

The discussion in the preceding paragraphs is meant as a rough, semiquantitative argument, for instance, the energy barrier ΔE_b does not only depend on the structure factor of the

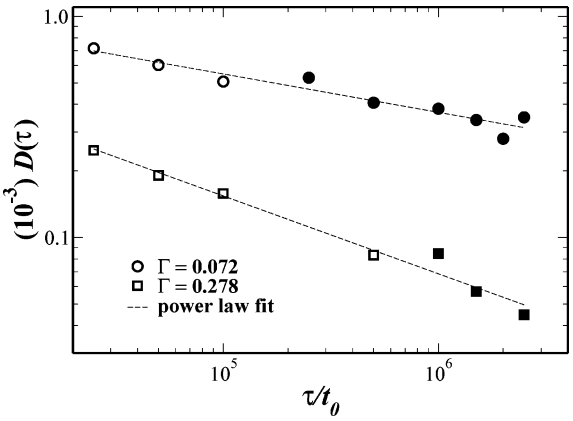

Figure 9. Aging of the lateral diffusion coefficient with the relaxation time at two different surface coverage concentrations Γ. The lines are fit according to the eq 11. Solid symbols refer to data in which the islands have merged completely, while open symbols reflect disconnected islands.

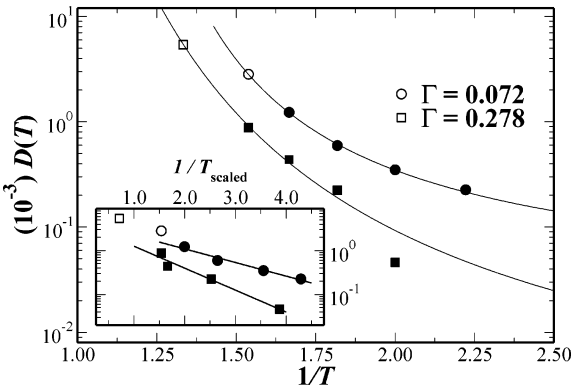

Figure 10. Diffusion coefficient D as a function of inverse of temperature for two different values of Γ. D is calculated for the sample of age $\tau = 2.5 \times 10^6 t_0$. The solid lines are guides to the eye. The inset shows D as a function of an inverse effective or scaled temperature $T_{scaled} = TS(G, T_{ref})/S(G, T)$, where T_{ref} was chosen to be 0.6 in LJ units. Closed symbols refer to regular structures. Open symbols indicate that either islands are disconnected (Γ = 0.072) at large T or that single layers were formed instead of double layers (Γ = 0.278).

first reciprocal lattice vector but also higher reciprocal lattice vectors. It is so much more surprising that the different rates of aging that we observe appear to be consistent with the suggested interlocking scenario, i.e., if we define the rate of aging in the diffusion constant as

$$R = \frac{\partial \ln D(\tau)}{\partial \ln \tau} \tag{12}$$

then we would expect R to be equal to $-\alpha S_0(G)/k_B T$. The value of $S_0(G)$ is approximately twice as large for the double layers than for the single layers (see Figure 2 in ref 22). This is consistent with a rate of aging shown in the Figure 9, which is twice as large for the double layer (Γ = 0.278) than for the single layer (Γ = 0.072).

It is worth pointing out that the aging of D sometimes (for instance in Figure 9) does not show cusps depending on whether the big island has formed already or not, while the time dependence of $S(G,\tau)$ is much more affected by the aggregation of small islands into one large islands. (Ideally one would evaluate $S(G,\tau)$ only for isolated islands, as this would reduce interference effects.) Thus, when plotting D as a function of $S(G)$, a cusp would become apparent at the point that separates disconnected islands from aggregated islands.

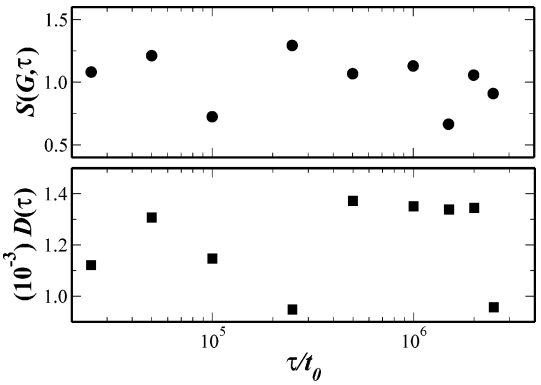

Figure 11. Time dependence of diffusion coefficient D for Γ = 0.072 and the structure factor S(Q) evaluated at the reciprocal lattice vector of the substrate. The Lennard-Jones radius for the interaction between substrate atoms and polymers is chosen to be $\sigma_{sp} = 1.25$, which decreases roughness but increases adhesion. No relaxational dynamics can be observed. The scatter of the data reflects our stochastic error bars.

3.5. Temperature Dependence at Default Surface Roughness. Equation 10 does not only relate the diffusion constant to the structure factor but also to the temperature. To further investigate the Arrhenius picture outlined in eqs 9 and 10, we calculated the temperature dependence of the island diffusion coefficient; see Figure 10. The bare data show strong deviation from Arrhenius-like behavior.

Deviation from Arrhenius laws are commonly related to the temperature dependence of free energy barriers. At smaller temperatures, the system can relax more deeply into the energy minima, and the motion of particles becomes more collective. In our case, we would expect that the relevant structural relaxation is the density modulation associated with a reciprocal lattice vector of the lattice. Thus, if our assumption is correct, the temperature dependence of the diffusion coefficient should become Arrhenius-like if we correct the temperature axis for the effect due to the temperature change in $S(G)$. This can be done by defining a scaled temperature $T_{scaled} = TS(G, T_{ref})/S(G, T)$, where T_{ref} is an arbitrary reference temperature, which we chose to be $T_{ref} = 0.65\epsilon/k_B$, ϵ being the LJ energy scale. Within the phenomenological model, eq 10 can now be rewritten as

$$D(T_{scaled}) = D_0 e^{-\tilde{E}/k_B T_{scaled}} \tag{13}$$

where $\tilde{E} = \alpha S(G, T_{scaled})$ is temperature independent. The "predicted'' Arrhenius behavior is clearly evidenced in the inset of Figure 10.

The simulations thus show that the glassy behavior of our model chain molecules is intimately linked to the way in which the substrate manages to imprint its corrugation in the adsorbed film. Layering of the polymers themselves, as a consequence of the confinement or semiconfinement, is insufficient to explain the glassy dynamics.

3.6. Effect of Substrate Corrugation: Smooth vs Rough Surface. In this section, we investigate how altering the corrugation affects the diffusion constant, the structure factor, and their time dependence. To reduce corrugation, the Lennard-Jones radius for the interaction between substrate and polymers, σ_{sp}, was increased from unity to $\sigma_{sp} = 1.25$. This makes the substrate effectively smoother and due to the longer range of the interaction more attractive. Thus, one may argue that the corrugation is decreased while the adhesion (or confinement) is increased. As can be seen in Figure 11, no relaxational dynamics can be ascertained for the case of reduced roughness

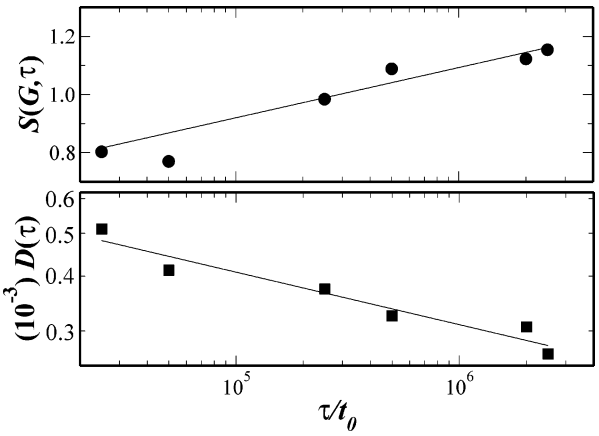

Figure 12. Time dependence of diffusion coefficient D for $\Gamma = 0.072$ and structure factor $S(Q)$ evaluated at the reciprocal lattice vector of the substrate G. The Lennard-Jones radius for the interaction between substrate atoms and polymers is chosen to be $\sigma_{sp} = 0.9$, which increases roughness but decreases adhesion. Lines are drawn to guide the eye.

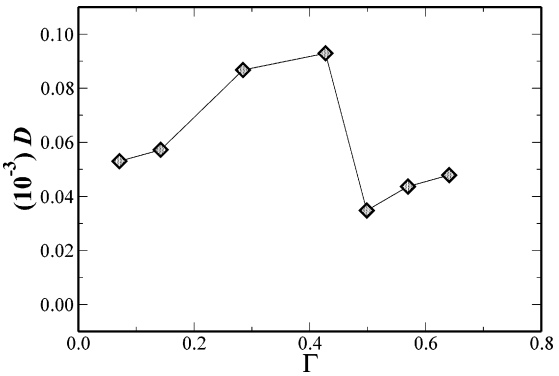

Figure 13. Lateral diffusion coefficient as a function of surface coverage Γ for the amorphous surface.

and increased confinement. Moreover, the mobility has increased with respect to the rougher substrate.

Opposite trends are observed when the roughness is increased rather than decreased. Results for $\sigma_{sp} = 0.9$ are depicted in Figure 12. The diffusion constant is now reduced with respect to the default configuration, e.g., at small times ($3 \times 10^4 t_0$), there is a 20% decrease in D. Because of the reduced mobility, the polymers cannot so quickly adopt their structure to the substrate, which explains why the structure factor for the rough substrate ($\sigma_{sp} = 0.9$) is initially smaller than that for the smooth substrate ($\sigma_{sp} = 1.25$). At very long times, however, the roughest substrate must be expected to have imprinted its corrugation more strongly than the two smoother surfaces.

The analysis presented here thus suggests that aging in the simulated films is intimately linked to substrate corrugation. The logarithmic aging of the structure factor and the power law aging with time of the diffusion coefficient disappears upon decreased corrugation although adhesion and thus confinement are increased.

4. Results for Amorphous Surfaces

To investigate whether the symmetry of the substrate affects the observed Λ-shape anomaly qualitatively, disordered substrates were investigated as well. Disordered surfaces were generated using the protocol described in section 2. Linear dimensions of the surface, thermal energy, and deposition algorithm were similar as for crystalline surfaces.

Results for D as a function of Γ are shown in Figure 13. The same trend is followed here as for crystalline surfaces, i.e., there

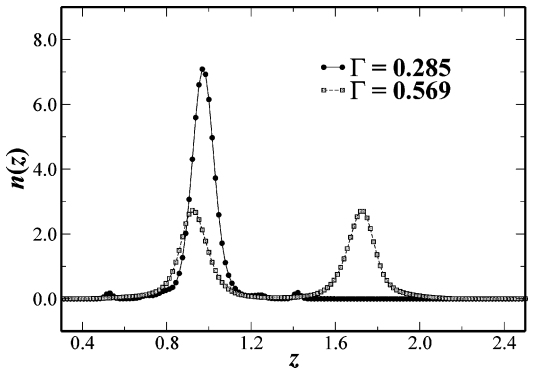

Figure 14. Density of the monomers $n(z)$ as a function of the distance z from the amorphous substrate.

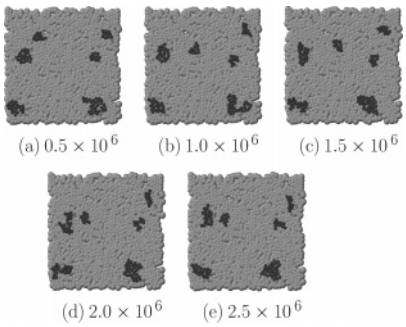

Figure 15. Molecular snapshots showing the time evolution of the adsorbed films on amorphous surface for $\Gamma = 0.072$ at the indicated age τ/t_0.

is first an increase in D with Γ at small Γ, followed by an abrupt decrease of D at a threshold concentration $\Gamma^* = 0.4$. The value for Γ^* in our disordered model is approximately twice as large as that for the crystalline substrates. The larger value in the amorphous case can be rationalized as follows: In order to have an essentially impenetrable surface, more wall atoms per surface area have to be included in the amorphous case as compared to the crystalline case. This increases the adhesion and thus the propensity of adsorbing polymers to form single-layer structures.

As before, the discontinuity of D at Γ^* is due to a structural transition from single layers to double layers, see Figure 14. This is not unexpected as the argument that double layers can more easily pin into the substrate corrugation than single layers is based on local arguments and thus does not require long-range order.

Besides the difference in Γ^* between amorphous and crystalline walls, it appears that (a) the diffusion constant is smaller in the amorphous case, and (b) the relative reduction of D at Γ^* is less dramatic for the disordered system than for the ordered system. Point a can be explained by the fact that amorphous walls are rougher than crystalline walls and thus provide larger energy barriers to diffusive motion. Point b may be rationalized by the heterogeneous distributions of island size in the amorphous case.

Because of the smaller diffusion constants, it takes much longer on disordered surfaces for the islands to join. One may argue that, owing to disorder, the substrate can pin individual islands more easily. While on average, the system is translationally invariant, locally the disordered systems are lacking symmetry and thus, there may be locations on the surface, where adsorption is more favorable than at others. Investigating the time evolution of structures, see Figure 15, does not reveal very clearly which islands may be pinned. However, it does become obvious that the measured diffusion constant is dominated by

the motion of a few small islands. We had to abstain from a more detailed analysis for disordered substrates, because a systematic disorder average analysis would have been computationally infeasible at present, despite the model's simplicity.

5. Conclusions

We have performed MD simulations of a generic model for polymer diffusion on surfaces to unravel the origin of (a) glassy dynamics of polymers in (semi)-confinement,[28] and (b) to further elucidate the anomalous increase increase of lateral mobility with the increasing Γ at a small surface coverage.[22] While our simple bead spring model certainly does not address many details of the experimental systems, it does qualitatively reproduce many experimental features, such as the power law aging of the diffusion constant with time, logarithmic aging of the structure factor, an increase of D with Γ at small Γ, and a sudden drop of D at a threshold concentration Γ^*. While the present study was concerned with chain molecules of fixed degree of polymerization N and varying surface coverages, the same model also reproduces the correct scaling behavior of D with N depending on whether the substrate is solid or fluid.[16] We are thus confident that the model is appropriate to investigate the generic dynamical features of chain molecules that are strongly adsorbed on surfaces.

As for point a, we could show that the glassy dynamics are not (only) due to layering but (also) to the way in which the substrate manages to imprint a density modulation in the adsorbed layer; i.e., the diffusion constant is an exponential function of inverse temperature times the structure factor evaluated at the substrate's smallest, nonzero reciprocal lattice vector. When the interactions are altered in a way that corrugation is decreased but adhesion and thus confinement increased, the mobility of the polymers increases. It is thus clear that the breaking of in-plane translational invariance is more important than the out-of-plane translational invariance ("confinement'', layering, etc.)

As for point b, our model shows that D decreases with Γ at small Γ if the monomers' z-components are fixed, while D increases when they are unconstrained. When Γ is increased, fluctuations normal to the surface in single-layered structures become more dominant, and these normal fluctuations allow the monomers to cross the corrugation barriers more easily than if there are no such fluctuations. Thus, the increase of D with Γ at small Γ is due to the increased fluctuations normal to the surface, at least in our model system. Once the fluctuations are so large that double layers form, i.e., for $\Gamma > \Gamma^*$, the adsorbed films lock more easily into the substrate's corrugation resulting in a sudden decrease of D.

Validating the scenarios presented here for specific systems will certainly require chemically detailed simulations. This is currently beyond our computational feasibilities. The bottleneck is the immense number of time steps required to obtain meaningful averages.

Acknowledgment. We thank the Ontario Ministry of Energy and the Natural Science and Engineering Research Council of Canada for financial support. We also thank the Colin Denniston group for making available their computer cluster at UWO and WESTGRID supercomputing facility, where part of the computation was performed.

References and Notes

(1) de Gennes, P.-G. *Scaling Concepts in Polymer Physics*; Cornell University Press: London, 1979.
(2) Doi, M.; Edwards, S. F. *The Theory of Polymer Dynamics*; Clarendon Press: Oxford U.K., 1986).
(3) Kremer, K.; Grest, G. S.; Carmesin, I. *Phys. Rev. Lett.* **1988**, *61*, 566.
(4) Dünweg, B.; Kremer, K. *Phys. Rev. Lett.* **1991**, *66*, 2996.
(5) Milchev, A.; Binder, K. *Macromolecules* **1996**, *29*, 343.
(6) Sukhishvili, S. A.; Chen, Y.; Müller, J. D.; Schweizer, K. S.; Gratton, E.; S. Granick, *Nature* **2000**, *406*, 146.
(7) Sukhishvili, S. A.; Chen, Y.; Müller, J. D.; Gratton, E.; Schweizer, K. S.; Granick, S. *Macromolecules* **2002**, *35*, 1776.
(8) Shaughnessy, B. O'; Vavylonis, D. *J. Phys.: Cond. Mat.* **2005**, **17**, R63.
(9) Patel, S. S.; Tirrel, M. *Annu. Rev. Phys. Chem.* **1989**, *40*, 597.
(10) Granick, S.; et. al. *J. Polym. Sci. B* **2003**, *41*, 2755.
(11) Azuma, R.; Takayama, H. *J. Chem. Phys.* **1999**, *111*, 8666.
(12) Falck, E.; Punkkinen, O.; Vattulainen, I.; Ala-Nissila, T. *Phys. Rev. E* **2003**, *68*, 50102.
(13) Lai, P. Y. *Phys. Rev. E* **1994**, *49*, 5420.
(14) Klein Wolterink, J.; Barkema, G. T.; Cohen Stuart, M. A. *Macromolecules* **2005**, *38*, 2009.
(15) Desai, T. G.; Keblinski, P.; Kumar, S. K.; Granick, S. *J. Chem. Phys.* **2006**, *124*, 084904.
(16) Mukherji, D.; Bartels, G.; Müser, M. H. *Phys. Rev. E* (submitted).
(17) Bae, S. C.; Xie, F.; Jeon, S.; Granick, S. *Curr. Opin. Solid State Mater.* **2001**, *5*, 327.
(18) Liu, R. G.; Gao, X.; Adams, J.; Oppermann, W. *Macromolecules* **2005**, *38*, 8845.
(19) Maier, B.; Rädler, J. O. *Phys. Rev. Lett.* **1999**, *82*, 1911.
(20) Maier, B.; Rädler, J. O. *Macromolecules* **2000**, *33*, 7185.
(21) Zhao, J.; Granick, S. *J. Am. Chem. Soc.* **2004**, *126*, 6242.
(22) Mukherji, D.; Müser, M. H. *Phys. Rev. E* **2006**, *74*, 10601.
(23) Smith, E. D.; Robbins, M. O.; Cieplak, M. *Phys. Rev. B* **1996**, *54*, 8252.
(24) Persson, B. N. J.; Nitzan, A. *Surf. Sci.* **1996**, *367*, 261.
(25) Robbins, M. O.; Müser, M. H. In *Nanotribology Handbook*; Bhushan, B., Ed.; Springer-Verlag: Berlin, 2004.
(26) Weeks, E. R.; Crocker, J. C.; Levitt, A. C.; Schofield, A.; Weitz, D. A. *Science* **2000**, *287*, 627.
(27) Torre, R.; Bartolini, P.; Righini, R. *Nature* **2004**, *428*, 296.
(28) Priestly, R. D.; Ellison, C. J.; Broadbelt, L. J.; Torkelson, J. M. *Science* **2005**, *309*, 456.
(29) Struik, L. C. E. *Physical Aging in Amorphous Polymers and Other Materials*; Elsevier: New York, 1978.
(30) Hutchinson, J. M. *Prog. Polym. Sci.* **1995**, *20*, 703.
(31) Frantz, P.; Granick, S. *Phys. Rev. Lett.* **1991**, *66*, 899.
(32) Pfromm, P. H.; Koros, W. J. *Polymer* **1995**, *36*, 2379.
(33) Huang, Y.; Paul, D. R. *Macromolecules* **2006**, *39*, 1554.
(34) Huang, Y.; Paul, D. R. *Macromolecules* **2005**, *38*, 10148.
(35) He, G.; Robbins, M. O. *Tribology Letters* **2001**, *10*, 7.
(36) Kremer, K.; Grest, G. S. *J. Chem. Phys.* **1990**, *92*, 5057.
(37) Kröger, M. *Phys. Rep.* **2004**, *390*, 453.
(38) Müser, M. H.; Wenning, L.; Robbins, M. O. *Phys. Rev. Lett.* **2001**, *86*, 1295.
(39) Müser, M. H.; Robbins, M. O. *Phys. Rev. B* **2000**, *61*, 2335.

MA0627370